energies

MDPI

Article

Comprehensive Benefit Evaluation of Residential Solar and Battery Systems in Japan Considering Outage Mitigation and Battery Degradation

Masashi Matsubara *, Masahiro Mae and Ryuji Matsuhashi

Department of Electrical Engineering and Information Systems, The University of Tokyo, Tokyo 113-8656, Japan; mae@enesys.t.u-tokyo.ac.jp (M.M.); matu@enesys.t.u-tokyo.ac.jp (R.M.)
* Correspondence: matsubara@enesys.t.u-tokyo.ac.jp

Abstract

Residential photovoltaic and battery energy storage systems (PV/BESS systems) are gaining attention as a measure against natural disasters and rising electricity prices. This paper aims to propose an operational strategy that balances electricity cost reductions, battery lifespans, and outage mitigation for the residential PV/BESS system. The optimization model considering battery degradation determines normal operations with balancing cost reductions and degradation. Additionally, a rule-based approach simulates system performance during various outages and evaluates supply continuity using a resilience metric: the percent continuous supply hour. Outage mitigation benefits are quantified by considering the distribution of residential values of lost load (VoLLs). Results show that the operation considering degradation maintains a high state of charge (SoC) at all times. For 25.7% of households with large demand, electricity cost reductions exceed equipment costs. Outage simulations demonstrate that the mean energy supplied during a 48-h outage ranges from 14 kWh to 26.7 kWh. Furthermore, the proposed operation increases the resilience metric from 20% to 30% under severe and unpredictable outages. Finally, incorporating outage mitigation benefits increases the proportion of households adopting PV/BESS systems by 21.5% points.

Keywords: battery degradation; economic analysis; outage simulation; residential resilience; supply continuity; value of lost load

Academic Editors: Kwok Tong Chau and Jiaqiang E

Received: 21 November 2025
Revised: 5 December 2025
Accepted: 13 December 2025
Published: 16 December 2025

1. Introduction

Blackouts caused by natural disasters are becoming more frequent and severe. For example, Typhoon No. 15 (Faxai) in 2019 caused a widespread and prolonged blackout in the Tokyo region [1], while a severe winter storm in Texas caused the loss of 30 GW of generation capacity and a large-scale blackout in February 2021 [2]. In Japan, major earthquakes such as the Great East Japan earthquake [3], the Hokkaido Eastern Iburi Earthquake [4], and the Noto Peninsula Earthquake in 2024 have also triggered extensive blackouts. Although power system operators strive to enhance grid resilience, they cannot practically prevent all blackouts . Thus, electricity consumers need to adopt self-defensive measures to prepare for and mitigate power outages.

In addition to the growing risk of emergencies, electricity prices have been rising due to increasing fossil fuel costs. During the winter of 2022, energy prices rose significantly across many regions, driven by geopolitical disruptions [5]. This highlighted the significance of

energy security, including improving self-sufficiency rates [6]. In Japan, retail electricity prices rose sharply after the winter of 2022, directly impacting households. Consequently, residential systems that enhance self-sufficiency have attracted greater attention as a means to mitigate rising costs.

A combination of photovoltaics and battery energy storage systems (PV/BESS systems) offers a promising solution to address both increasing outages and rising electricity costs. PV/BESS systems promote self-consumptions and provide backup power during blackouts [7]. In Japan, residential PV installations expanded rapidly after the Great East Japan Earthquake in 2011, reaching 11 GW by October 2024. The feed-in tariff (FIT) program initially supported PV adoption by allowing households to sell generation at a constant price for 10 years, enabling cost recovery. However, FIT rates have declined, and many households have completed their FIT contracts. As a result, maximizing self-consumptions through PV generation combined with batteries become the primary source of benefit. However, high investment costs remain a major barrier to PV/BESS system adoption. Thus, the residential benefits of PV/BESS systems should be investigated to promote their wider deployment.

Several papers have investigated the PV/BESS system in terms of cost reductions and self-sufficiency. Previous research has analyzed economic benefits related to demand smoothing [8], self-consumptions in various regions [9], integration with flexible loads [10], and reductions in contract capacity [11]. Economic efficiency has been discussed through the optimization of system sizes [11] and comparisons with hydrogen-based systems [12]. When combined with home energy management, user preferences and cost reductions can be optimized simultaneously [13]. Although households can benefit economically from PV/BESS systems, batteries are often not cost-effective under residential usage patterns [8,14]. Deep charge and discharge cycles can achieve greater cost reductions but accelerate battery's degradation, shortening its lifespan and increasing replacement costs. Furthermore, deep discharge increases vulnerability to sudden supply interruptions due to insufficient stored energy. To balance cost reductions and battery lifespans, several papers have proposed operations that minimize degradation [14–16]. However, a comprehensive evaluation of outage mitigation and cost reduction benefits, including resilience aspects, remains limited.

Many studies have investigated measures taken by power system operators to prevent and mitigate supply interruptions. Wang et al. [17] categorizes these measures into prevention, mitigation, and recovery. Preventive measures include expanding distribution networks [18], reinforcing transmission lines [19], installing batteries [20,21] and electric vehicles [22], and tree trimming [23]. Mitigation measures aim to limit the spread of interruptions, such as disconnection of transmission lines [24,25], microgrid deployment [3,26–28], and charge control of distributed electric vehicles [29]. Recovery time can be shortened by optimizing repair crew dispatch and movable generator allocation [30]. From a residential perspective, these measures reduce the frequency of outages in households.

Previous research has also explored residential PV/BESS systems primarily for outage mitigation. Key topics include optimal sizing, operational strategies, and economic feasibility. Papers on sizing have investigated minimizing total costs including outage damage [31], mitigating multi-day outages [32], case studies on hurricanes in the U.S. [33], comparisons with natural gas generators [34], and planning methods based on reliability indices [35]. Operational strategies for outage mitigation aim to prepare for unpredictable outages [36] and integrate electric vehicles [37] and flexible loads [38]. Some papers have analyzed coordination among households with distributed PV/BESS systems [39] and shared systems [40,41]. Outage mitigation can motivate households to adopt PV/BESS systems, and several papers have quantified its benefits considering regional differences [42],

integration with flexible load control [43], and unpredictable outages [36]. These studies evaluate resilience using the amount of energy supplied during outages. However, supply continuity for critical loads remains underexplored. Even short outages can cause severe discomfort, such as rising indoor temperatures [44], and may threaten lives by interrupting medical equipment [45]. Thus, supply continuity is crucial for resilience.

The economic value of outage mitigation can be quantified using the value of lost load (VoLL) [46,47], which represents the cost of unserved energy during outages. Residential VoLLs have been estimated in various countries, including the U.S. [48,49], Norway [50], Korea [51], and Japan [52]. Several papers have converted outage mitigation into benefits in buildings [53] and households using historical outages [42]. They have used a representative VoLL values for conversion [36,42,43,53]. However, VoLLs vary widely among households [50–52], influencing PV/BESS system adoption. The impact of this distribution on benefit evaluation remains underexplored. A more detailed analysis is needed to assess how outage mitigation benefits differ among households with varying VoLLs.

Power systems face increasing risks of large-scale supply interruptions and rising energy costs. Residential PV/BESS systems have the potential to mitigate these risks. To maximize their benefits, it is essential to balance cost reductions, battery degradation management, and outage mitigation. However, there is a trade-off: aggressive battery cycling reduces electricity costs but accelerates degradation and increases vulnerability to sudden supply interruptions. A comprehensive analysis of economic efficiency, battery degradation, and outage mitigation of PV/BESS systems has yet to be fully conducted. This paper aims to propose an operation of residential PV/BESS systems that addresses all these aspects. The operation minimizes the sum of annual electricity costs and battery degradation costs, ensuing that batteries maintain a high state of charge (SoC) to enhance resilience. This paper evaluates the balance between cost reductions, outage mitigation, and equipment costs under the proposed operation. Additionally, this paper evaluates supply continuity during outages. The duration for which the PV/BESS system can continue to serve critical loads is assessed under different battery's operations.

The contributions of this paper are as follows:

- It evaluates electricity cost reductions and PV/BESS equipment costs through optimization explicitly considering battery degradation.
- It simulates operations during outages and evaluates supply continuity for critical loads.
- It combines outage mitigation benefits with economic efficiency, considering the distribution of residential VoLLs.

The remainder of this paper is organized as follows. The method to determine operations and analyze outage mitigation are explained in Section 2. The simulation results are explained in Section 3. At last, the conclusion is explained in Section 4.

2. Method

This paper simulates annual operations of residential PV/BESS systems using an optimization model and evaluates outage mitigation through a rule-based algorithm. Figure 1 shows the overall procedure. The inputs include the household and outage data. The optimization problem determines the SoC and electricity cost reductions by PV/BESS systems. The outage simulations determine energy supplied and continuous supply hours for critical loads during outages. The SoC information affects the initial state when a sudden outage occurs. The analysis combines economic efficiency and resilience by converting outage mitigation into economic benefits using the residential VoLL.

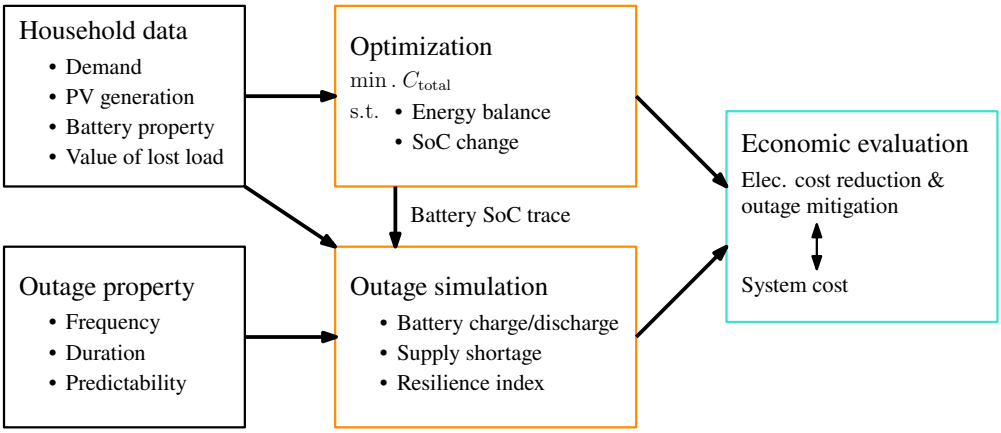

Figure 1. Overall procedure in the simulation of residential photovoltaic and battery energy storage systems (PV/BESS systems). Black arrows show the data flows.

2.1. Household Model

Figure 2 shows the household model. The household has a battery and rooftop solar panels. The battery has a 5 kW charge and discharge output and a 13.5 kWh capacity. Its one-way efficiency is 90% in charging and discharging. Its SoC operates between 10% and 90%. The PV system has a 3 kW capacity. Its generation profile is based on annual global horizontal irradiance data in Osaka, Japan [54], as shown in Figure 3.

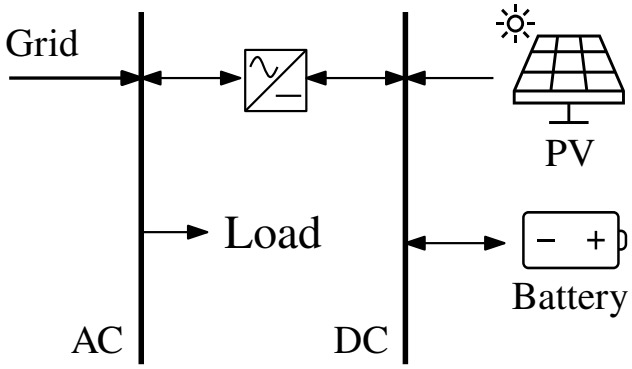

Figure 2. Household electricity model.

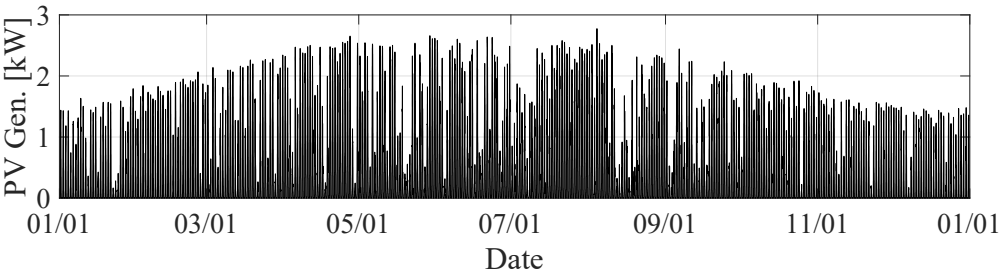

Figure 3. Annual generation profile of the 3 kW PV system.

Electricity prices follow the wholesale market prices in the Kansai region [55]. Figure 4 shows the electricity prices. The prices are updated one day before the actual supply and vary in every 30 min. Fluctuated prices can promote electricity cost reductions by the PV/BESS system.

This paper uses demand data from 70 households in the Kansai region in Japan. The identical PV and battery sizes are applied to all households for comparison. PV generation is the same in all households.

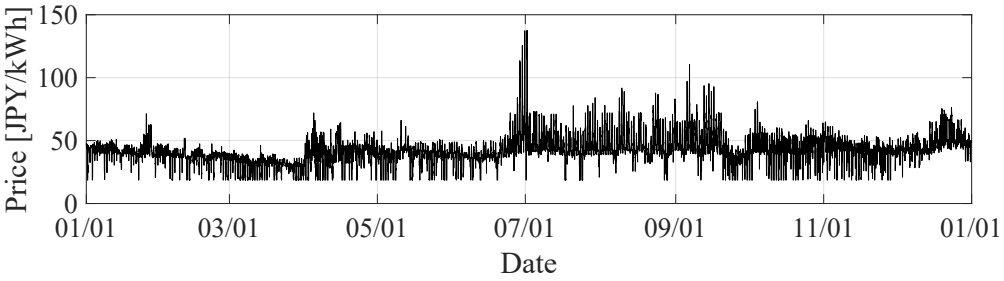

Figure 4. Annual electricity variable prices [55].

2.2. Battery Degradation Model

Battery degradation occurs due to charge/discharge cycles, which is called the cycle effect. The degradation includes the capacity fade and power fade. This paper focuses on the capacity fade because the capacity reduction significantly impacts operation. This paper uses a model based on [56]. The model in [56] shows the cycle effect as (1).

$$\xi_{\text{deg}}(SOC_{\text{ave}}, SOC_{\text{dev}}) = k_1 SOC_{\text{dev}} \exp[k_2 SOC_{\text{ave}}] + k_3 \exp[k_4 SOC_{\text{dev}}]. \quad (1)$$

This model shows that degradation in a cycle depends on an average SoC (SOC_{ave}) and an SoC deviation (SOC_{dev}). ξ_{deg} denotes the capacity fade. k_1, k_2, k_3, and k_4 denote the parameters, as shown in Table 1. This paper converts the average SoC and SoC deviation to a bottom SoC (SOC_{bottom}) in a complete cycle using Equations (2) and (3). Thus, the degradation model can be described as (4).

$$SOC_{\text{ave}} = \frac{1 + SOC_{\text{bottom}}}{2}. \quad (2)$$

$$SOC_{\text{dev}} = \frac{1 - SOC_{\text{bottom}}}{2}. \quad (3)$$

$$\xi_{\text{deg}}(SOC_{\text{bottom}}) = k_1 \frac{1 - SOC_{\text{bottom}}}{2} \exp\left[k_2 \frac{1 + SOC_{\text{bottom}}}{2}\right] + k_3 \exp\left[k_4 \frac{1 - SOC_{\text{bottom}}}{2}\right]. \quad (4)$$

Figure 5 shows the relationship between the bottom SoC in a complete cycle and the degradation amount. A battery capacity degrades fast with deep discharge.

Table 1. Parameters in the battery degradation model [56].

k_1	k_2	k_3	k_4
-4.092×10^{-4}	-2.167	1.408×10^{-5}	6.130

The degradation amount is non-linear against the SoC change. It is discretized into eight segments for piecewise linearization. Each segment has the width of a 10% SoC. The endpoints are set between 10% and 90% following the battery operation range. A red dashed line in Figure 5 shows the linearized degradation amount in a complete cycle.

Battery degradation also occurs regardless of charge/discharge cycles, which is called the calendar effect. The calendar effect depends on the years of use, temperature, and SoC [16]. For simplicity, it reduces the battery capacity by 1.2%/year regardless of temperature and SoC based on experimental results [57].

The cumulative degradation determines the battery lifespan. This paper assumes that the battery lifespan ends when capacity decreases by 30%. The degradation and lifespan of solar panels are not considered.

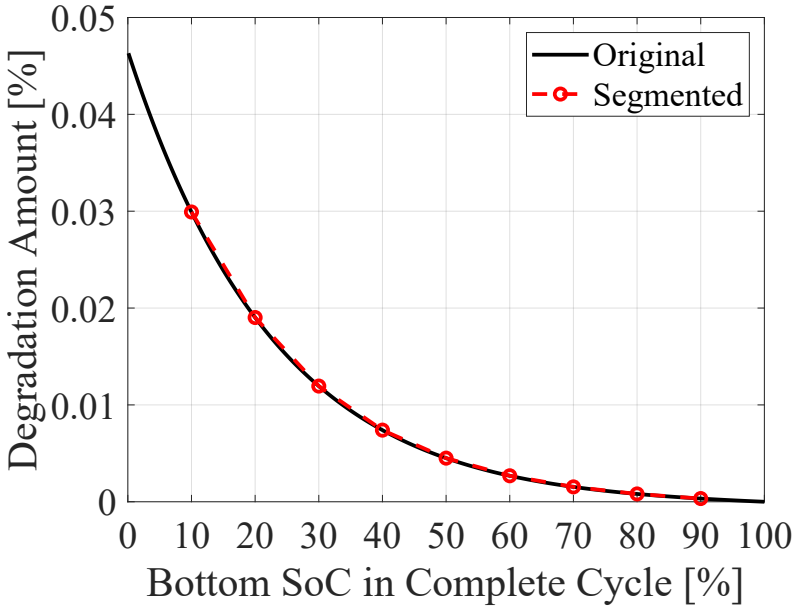

Figure 5. Degradation amount per complete cycle and its piecewise linear approximation.

2.3. Optimization for Normal Operation

The optimization problem decides the battery's normal operation. Table 2 shows the nomenclature of symbols used in the following equations. The optimization minimizes the total annual cost shown in (5). It includes electricity and degradation costs to balance electricity cost reductions and battery lifespans. Electricity costs ($C_{\mathrm{elec},t}$) depend on time-varying prices, as shown in (6). Excess energy of PV generation ($C_{\mathrm{sell},t}$) can sell at 15 JPY/kWh in the first 10 years based on the FIT scheme and 8 JPY/kWh in the rest based on the retail contract. Its sale ($C_{\mathrm{sell},t}$) is calculated as (7).

$$C_{\mathrm{total}} = \sum_t \Big(C_{\mathrm{elec},t} + C_{\mathrm{deg},t} - C_{\mathrm{sell},t} \Big). \tag{5}$$

$$C_{\mathrm{elec},t} = \sum_t UC_{\mathrm{elec},t} \times E_{\mathrm{grid},t}. \tag{6}$$

$$C_{\mathrm{sell},t} = \sum_t UC_{\mathrm{sell},t} \times E_{\mathrm{sell},t}. \tag{7}$$

The degradation cost is calculated from degradation amounts, the battery's lifespan, and the battery's equipment costs. Its definition is shown in (8).

$$C_{\mathrm{deg},t} = C_{\mathrm{inv,BT}} \frac{D_t}{1 - SOH^{\min}}. \tag{8}$$

Degradation amounts are calculated using the method in [58]. It concentrates degradation in discharging processes. In other words, degradation costs happen only in discharging in the optimization. Constraints (9) and (10) demonstrate the degradation. $\bar{\xi}_{\mathrm{deg}}$ denotes the linearized degradation amount in a complete cycle, as shown in a red dashed line in Figure 5. The right-hand side of (9) becomes negative when charging, and vice versa. Constraint (10) limits the degradation amount to be non-negative. Hence, the degradation amount becomes positive only when the battery discharges.

$$D_t \geq \bar{\xi}_{\mathrm{deg}}(SOC_t) - \bar{\xi}_{\mathrm{deg}}(SOC_{t-1}). \tag{9}$$

$$D_t \geq 0. \tag{10}$$

Table 2. Nomenclature of symbols in the optimization definition.

Symbol	Definition	Unit
t	Time Slot	[-]
Variables		
C_{total}	Total cost	[JPY]
$E_{\text{grid},t}$	Supply from grid	[kWh]
$E_{\text{sell},t}$	Sold excess electricity to grid	[kWh]
$E_{\text{BTc},t}$	Consumption at battery charge	[kWh]
$E_{\text{BTd},t}$	Supply from battery discharge	[kWh]
$u_{\text{BTc},t}$	Battery charging state	0 or 1
SOC_t	Battery state of charge (SoC)	[-]
D_t	Battery degradation amount	[-]
Constants		
$UC_{\text{elec},t}$	Electricity variable price	[JPY/kWh]
$UC_{\text{sell},t}$	Excess electricity price	[JPY/kWh]
$E_{\text{dem},t}$	Demand	[kWh]
$E_{\text{PV},t}$	PV generation	[kWh]
$E_{\text{grid}}^{\max}$	Maximum supply from grid	[kWh]
$E_{\text{BT}}^{\max}$	Maximum output at battery	[kWh]
$SOC^{\min}$	Minimum SoC	[-]
$SOC^{\max}$	Maximum SoC	[-]
SOC^{margin}	SoC margin	[-]
CAP_{BT}	Battery capacity	[kWh]
η_{BT}	Battery charge/discharge efficiency	[-]
$C_{\text{inv,BT}}$	Battery equipment cost	[JPY]
$SOH^{\min}$	Battery capacity rate at the end of lifespan	[-]
$\bar{\xi}_{\text{deg}}$	Linearized degradation curve	[-]

The constraints in the optimization problem are described as follows:

$$E_{\text{grid},t} + E_{\text{PV},t} - E_{\text{sell},t} + E_{\text{BTd},t} = E_{\text{dem},t} + E_{\text{BTc},t}. \tag{11}$$

$$0 \leq E_{\text{grid},t} \leq E_{\text{grid}}^{\max}. \tag{12}$$

$$0 \leq E_{\text{sell},t} \leq E_{\text{PV},t}. \tag{13}$$

$$0 \leq E_{\text{BTc},t} \leq E_{\text{BT}}^{\max} \times u_{\text{BTc},t}. \tag{14}$$

$$0 \leq E_{\text{BTd},t} \leq E_{\text{BT}}^{\max} \times (1 - u_{\text{BTc},t}). \tag{15}$$

$$SOC_t \times CAP_{\text{BT}} = SOC_{t-1} \times CAP_{\text{BT}} + E_{\text{BTc},t} \times \eta_{\text{BT}} - E_{\text{BTd},t}/\eta_{\text{BT}}. \tag{16}$$

$$SOC^{\min} \leq SOC_t \leq SOC^{\max}. \tag{17}$$

Constraint (11) sets the supply and demand balance of electricity. Constraint (12) sets the upper limit of the grid supply. Constraint (13) limits sold energy so that it does not exceed the PV generation. Constraints (14) and (15) set the maximum charge and discharge. Charge and discharge cannot happen simultaneously, as the binary variable u_{BTc} describes. Constraint (16) sets the SoC change. Constraint (17) sets the maximum and minimum SoC to protect the battery.

The optimization problem is defined as follows:

$$\begin{aligned} &\min . \ (5) \\ &\text{s.t. } (6)\text{–}(17). \end{aligned}$$

It is a mixed-integer linear programming problem. It decides battery operations, power from the grid, and sold energy.

This paper also models operations without explicitly considering degradation for comparison. In this case, the problem minimizes electricity costs, as shown in (18). Additionally, the constraint (17) is changed to (19). The battery has the operational minimum SoC ($SOC^{\min}$). In (19), SOC^{margin} increases the minimum SoC to restrict deep discharge. This paper calls SOC^{margin} a "SoC margin" or just a "margin." An expression "margin X%" demonstrates that SOC^{margin} equals X%.

$$C_{\text{total}} = \sum_t (C_{\text{elec},t} - C_{\text{sell},t}). \tag{18}$$

$$SOC^{\min} + SOC^{\text{margin}} \leq SOC_t \leq SOC^{\max}. \tag{19}$$

Thus, the optimization problem without explicitly considering degradation is defined as follows:

$$\begin{aligned} &\min . \ (18) \\ &\text{s.t. } (6), (11)\text{–}(16), (19). \end{aligned}$$

In all optimization problems, the time resolution is 30 min.

Electricity prices affects the optimal operation, but households does not know future prices. This paper adopts a sliding window approach to handle this limitation. Figure 6 shows the optimization and operation procedure. In the afternoon of day $d-1$, households receive the prices in the following day (day d) and then determine the operation for that day. Each optimization problem covers two days, day d and $d+1$ (optimization window), to avoid the terminal effect, while only the operation for day d (operation window) is implemented. It is assumed that households can accurately forecast prices for day $d+1$. In the next optimization, the SoC at the end of day d is taken over to the initial SoC for day $d+1$, following constraint (16). Thus, annual operations are decided by sequential optimization, with the final SoC on the last day linked to the initial SoC on the first day.

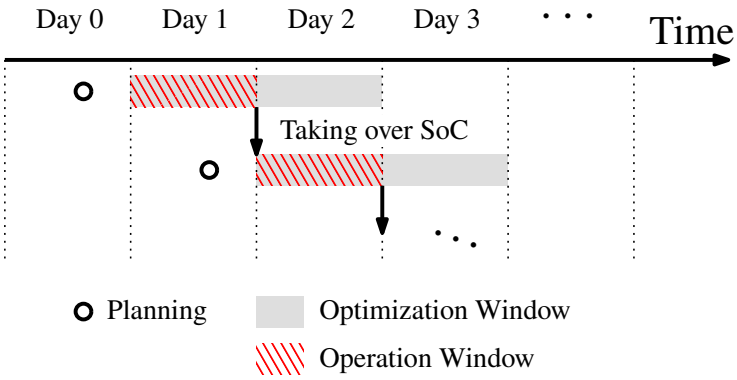

Figure 6. Optimization and operation procedure. The procedure is repeated day by day, as abbreviated by dots.

2.4. Outage Mitigation

2.4.1. Supply Interruptions in Japan

Outage mitigation benefits depend on the outage frequency and duration. The Cabinet Office, Government of Japan, collects information on disasters [59]. In addition, the cross-regional coordination summarizes reliability indices, such as loss of load probability (LOLP) [60]. This paper assumes an outage frequency and duration based on these data.

Figure 7 shows the average duration and frequency of outages per household in the Kansai region. In most years, the duration is less than 10 min per household, and the frequency is approximately 0.1 times per household. The average frequency from 2001 to 2022 is 0.13 times per household. Peaks in Figure 7 correspond to large-scale supply interruptions by disasters. From 2001 to 2023, 10 supply interruptions affecting more than 100,000 households happened after large typhoons [59], as shown in Table 3. 100,000 households account for 1.1% of all households (9 million [61]) in the Kansai region. Thus, large-scale typhoons have caused supply interruptions roughly once every 2 to 3 years. This paper make assumptions of two outage frequencies: 0.13 times/year based on the historical average, and 0.33 times/year, reflecting the frequency of large-scale supply interruptions. In the latter case, it is assumed that typhoons become more severe and damage the entire grid in an area with the same probability of approach and landfall.

Table 3. Large supply interruptions in the Kansai region from 2000 to 2023 affected more than 100,000 households [59]. Durations represent the time required to restore 99% of affected households.

Name (Year)	Outage Households	Duration
Typhoon No. 16 (2004)	559,000 (total)	1 day
Typhoon No. 18 (2004)	340,300 (total)	2 days
Typhoon No. 23 (2004)	369,000 (total)	5 days
Heavy snowfall (2006)	697,200 (total)	4.5 h
Typhoon No. 18 (2009)	153,000 (total)	36 h
Typhoon No. 12 (2011)	194,000 (total)	9 days
Typhoon No. 11 & 12 (2014)	105,280 (total)	<1 day
Typhoon No. 21 (2017)	108,320 (maximum)	3 days
Earthquake in North Osaka (2018)	170,300 (maximum)	50 min
Typhoon No. 20 (2018)	149,000 (maximum)	14.5 h
Typhoon No. 21 (2018)	1,700,000 (maximum)	5 days

In Japan, earthquakes, torrential rains, and heavy snowfalls also caused supply interruptions. There were large earthquakes that caused widespread and prolonged supply interruptions, such as the Great Hanshin Earthquake in 1995. However, such an earthquake rarely happens. A large earthquake in the Nankai trough may cause enormous damage to the power system, but it is predicted to happen with around 80% probability in the next 30 years [62]. This probability is one-tenth smaller than that of large typhoons. Torrential rains and heavy snowfalls sometimes cause supply interruptions in the summer and winter. However, these interruptions affected no more than 100,000 households, except the heavy snowfall in 2006 [59]. Although those disasters rarely cause large-scale supply interruptions, they can cause sudden supply interruptions.

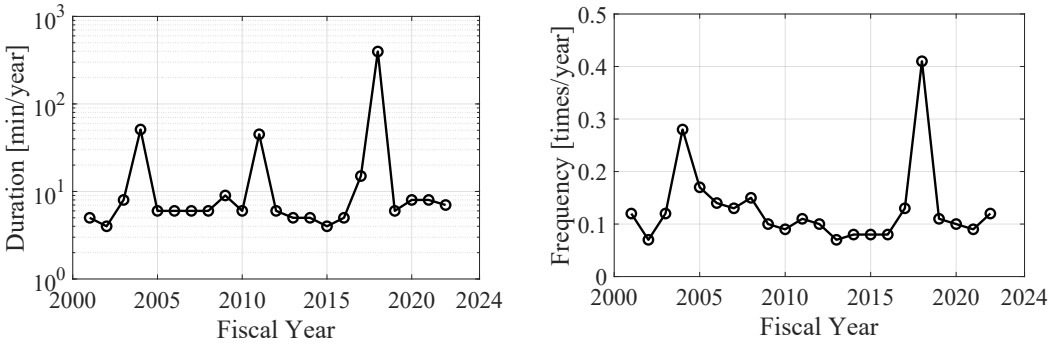

Figure 7. Historical power outages in the Kansai region [60]. (**Left**): average duration per household, (**right**): outage frequency or loss of load probability.

2.4.2. Supply Simulation During Outages

This paper simulates electricity supply by PV/BESS systems during outages. Electricity supply during prolonged outages depends on the start timings, durations, and predictability. The timing and duration affect the amount of PV generation. The predictability affects the energy stored in the battery before the outage.

This paper considers two types of outages: predictable outages and unpredictable outages. Table 4 shows the assumptions on outages. Outages caused by typhoons can be predicted by households. Thus, the battery has its maximum SoC (90%) before outages. Results in predictable outages decide outage mitigation benefits because almost all prolonged outages were caused by typhoons. Outages caused by earthquakes cannot be predicted. Thus, the initial SoC follows the SoC at an outage start timing, decided by optimization problems (Section 2.3). Thus, it does not necessarily equal the maximum SoC. Power supply is recovered 48 h after an outage happens. It is based on the median of durations in Table 3.

This paper focuses on outages in the summer (from July to September) because intense heat threatens lives. Outage mitigation in the winter is calculated for reference only, since hypothermia risks can be reduced by wearing warmer clothing and using fuels. The mitigation benefit is evaluated based on the energy supplied during predictable outages, given their relatively high frequency.

Various scenarios are generated by shifting the outage start timing by one-hour increments. Thus, 2208 scenarios (=92 [day] × 24 [h]) are generated for the summer. For the winter, 2160 scenarios (=90 [day] × 24 [h]) are generated. This paper simulates operations in each of 70 households.

Households may use critical loads during outages but suppress the other loads. Thus, PV/BESS systems serve electricity only to critical loads. The critical loads include refrigerators, air conditioners [52], plug loads, and lights [32]. This paper assumes power consumptions are 80 W for refrigerators, 500 W for air conditioners, 70 W for plug loads [32], and 50 W for lights. Lights are required in the evening and at night. Thus, the maximum critical loads are assumed to be 700 W in the evening (18:00–23:00) and 650 W at other times. If the normal demand is smaller than these values, the critical loads equal the normal demand.

A rule-based algorithm decides operations during outages. Figure 8 shows the procedure in a 30-min time step. $E^{\mathrm{c}}_{\mathrm{dem}}$ in Figure 8 denotes the critical loads. E_{supply} and E_{short} denote energy supplied and supply shortages. PV generation and battery discharge serve critical loads. If PV generation exceeds critical loads, the battery absorbs excess energy until its SoC reaches the maximum. The procedure is repeated until an outage ends. Finally, the simulation accumulates energy supplied and supply shortages.

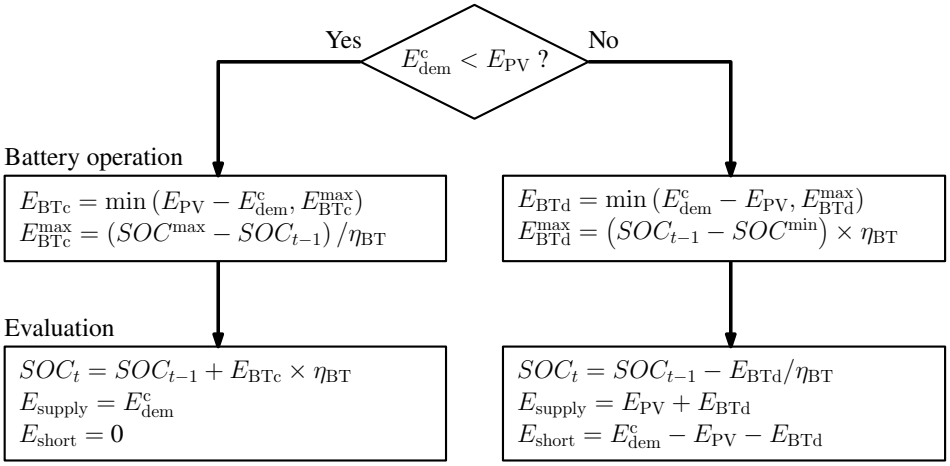

Figure 8. Rule-based procedure for outage simulation in each time step.

Solar power plants can be damaged by typhoons due to strong winds and heavy rain [63,64], as well as by earthquakes. For example, 3.5% of PV infrastructure on Hainan Island was damaged by Typhoon Yagi in 2024 [64]. However, the extent of damage to rooftop solar panels remains unclear in previous research. Thus, this paper assumes that rooftop solar panels can continue generating electricity after disasters.

Table 4. Outage assumptions in the simulation. "Summer" means June 1 to September 30, and "Winter" means December 1 to February 28. Winter outage results are excluded from benefit calculations due to their low occurrence.

Cause	Duration	Season	Initial SoC
Typhoons	48 h	Summer	SOC^{max} (90%)
Earthquakes	48 h	Summer	SOC_t in normal operations
Snowfalls	48 h	Winter	SOC^{max} (90%)

2.5. Evaluation of Simulations

2.5.1. Outage Mitigation Effects

The amounts of energy supplied and supply shortages are one of the resilience metrics [42]. However, resilience has transient aspects [65]. Hence, previous research has proposed resilience metrics. Resilience curves [66,67] are popular resilience descriptions. The area of curves [30,66] shows the total performance degradation. For transmission systems, performance degradation and recovery time have been quantified [24,25]. For microgrid resilience, outage frequencies, durations, and outage shortages have been proposed [68].

Continuing supply even in severe situations is one of the requirements for resilient systems. For example, continuous cooling is vital to avoid heatstrokes in the summer. To describe supply continuity during outages, this paper uses a metric: percent continuous supply hour. Figure 9 explains the concept of continuous supply hour. It is the maximum continuous length when critical loads are supplied. It ranges between zero to one, normalized by the outage duration.

The metric is calculated for each outage scenario in each household. This paper uses the median and worst 5% values of 2208 scenarios in each household. The worst 5% value shows mitigation effects in a severe case, such as outages at night.

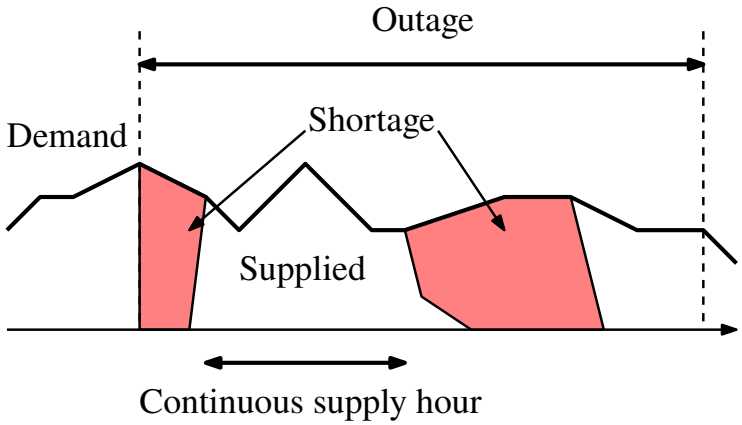

Figure 9. Concept of the continuous supply hour.

2.5.2. Economic Efficiency

The benefits of PV/BESS systems include electricity cost reductions and outage mitigation. Households adopt PV/BESS systems when these benefits exceed their costs. In the following equations, i denotes the household number, and k denotes the project year.

The costs and benefits are evaluated as net present values. The evaluation period is 20 years, based on the solar panel lifespan. Net present costs (NPC_i) include the investment costs, replacement costs, and electricity costs, as shown in (20). A discount rate (d) is 2% per year based on the nominal inflation rate in Japan. $C_{\text{inv,PV}}$ and $C_{\text{inv,BT}}$ denote the investment costs for the PV and battery. $C_{\text{rep,BT},k}$ denote the battery replacement costs in year k. The battery is replaced at the end of its lifespan defined by (21). The calendar effect (D^{cal}) equals 1.2% per year [57].

$$NPC_i = C_{\text{inv,PV}} + C_{\text{inv,BT}} + \sum_{k=1}^{20} \frac{C_{\text{rep,BT},k}}{(1+d)^k}. \tag{20}$$

$$L_{\text{BT},i} = \frac{1 - SOH^{\min}}{D^{\text{cal}} + \sum_t D_{i,t}}. \tag{21}$$

Net present benefits of cost reductions ($NPB_{\text{c},i}$) are defined in (22). $B_{\text{c},i}$ denotes the annual cost reduction calculated by the optimization results.

$$NPB_{\text{c},i} = \sum_{k=1}^{20} \frac{B_{\text{c},i}}{(1+d)^k}. \tag{22}$$

If the net present benefit of cost reductions exceeds the net present cost, a household adopts the PV/BESS system without outage mitigation. Otherwise, outage mitigation benefits can fill the gap between the equipment costs and electricity cost reductions.

Outage mitigation benefits depend on household's demand and VoLL. Annual mitigation benefits are calculated by (23).

$$B_{\text{miti},i} = \sum_t E_{\text{supply},i,t} \times VOLL_i \times f_{\text{outage}}. \tag{23}$$

$E_{\text{supply},i,t}$ denotes the mean energy supplied to critical loads [kWh] based on the summer outage simulations. f_{outage} denotes the outage frequency per year. VoLLs ($VOLL_i$) [JPY/kWh] vary in households. Previous work [52] demonstrates the distribution of residential VoLLs, as shown in Figure 10. It shows that 50% of households have 500 JPY/kWh or higher VoLLs, and a 10% of households have 4700 JPY/kWh or higher VoLLs. The expected proportion of households adopting the PV/BESS system is calculated by a breakeven VoLL. A breakeven VoLL is the minimum VoLL that achieves the total net present benefits exceeding the net present costs. It can be calculated as (24).

$$VOLL_i^{\text{b}} = \min\left(\frac{NPC_i - NPB_{\text{c},i}}{\sum_{k=1}^{20}(1+d)^k \times \sum_t E_{\text{supply},i,t} \times f_{\text{outage}}}, 0 \right). \tag{24}$$

$VOLL_i^{\text{b}}$ denotes the breakeven VoLL of household i. If cost reductions exceed equipment costs, it becomes zero. Then, an adoption probability in one household i is calculated by $\text{Prob}[T > VOLL_i^{\text{b}}] = P(VOLL_i^{\text{b}})$. $P(VOLL_i^{\text{b}})$ denotes the probability that VoLLs are larger than $VOLL_i^{\text{b}}$ (see Figure 10). If $VOLL_i^{\text{b}} = 0$, it becomes one. Hence, the expected proportion (R) is calculated as (25).

$$R = \frac{\sum_{i=1}^{N_{\text{house}}} P(VOLL_i^{\text{b}})}{N_{\text{house}}}. \tag{25}$$

N_{house} denotes the number of households.

The distribution of residential VoLLs depends on household attributes [50–52]. Previous work [52] suggests that monthly electricity bills influence VoLLs. Although this indicates a potential relationship between household demand and residential VoLLs, the

impact of demand has not been quantified. To the best of our knowledge, this quantitative effect remains unclear. Thus, this paper assumes that residential VoLLs are independent of demand.

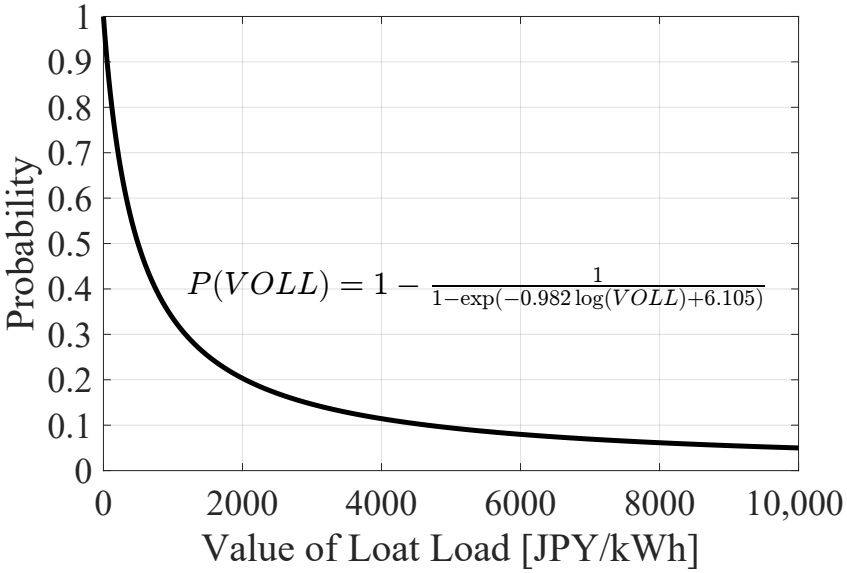

Figure 10. Probability distribution of residential value of lost load (VoLL) [52]. The vertical axis indicates the proportion of households with VoLL exceeding the corresponding value on the horizontal axis.

3. Result and Discussion

3.1. Operation in Normal States

Normal operations in 70 households are determined by mixed-integer linear programming problems. The problems are solved by the optimizer of Gurobi 12.0.1. The program was written by MATLAB R2024b. It was executed using a laptop computer with AMD Ryzen™ 7 8840U @ 3.30 GHz and 16.0 GB RAM @ 4800 MHz. It took around 5 min to simulate an annual operation in one household using the plugged-in laptop.

First, this paper compares the operation in one household determined by different optimization models. Annual average demand is 600 W, which is around the median of 70 households. Figure 11 shows the annual SoC profile with the operation considering degradation. The battery charges excess energy of PV generation and discharges at high electricity prices (see Figure 4). However, the battery avoids deep discharge because of significant degradation costs. As a result, the SoC stays higher than 60% most of the time. In contrast, Figure 12 shows the annual SoC profiles without considering degradation. If the battery can freely work (margin 0%), its SoC ranges from 10% to 90%. If the battery discharge is strictly limited (margin 60%), its SoC keeps higher than 70%. The battery operates more aggressively with the operation considering degradation than with a margin 60%.

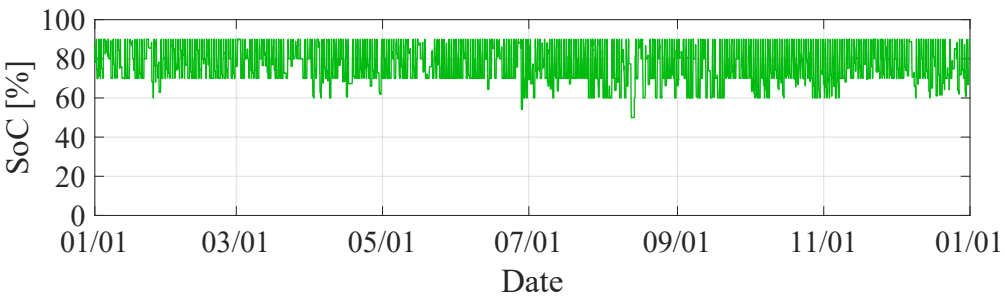

Figure 11. Annual state of charge (SoC) profile under the optimization considering degradation in one household.

Cost reductions and battery degradation depend on how deep the battery discharges. Table 5 shows annual electricity costs and degradation amounts. The degradation amount includes calendar and cycle effects. The PV/BESS system reduces electricity costs by 50–70% because of increased self-consumptions. Lower margins save more costs but accelerate degradation. Figure 13 compares cost reductions and equipment costs. The net present cost with a margin 0% reaches 7.73 $\times$ 10^6 JPY. Equipment costs decrease as the margin increases because of less battery replacement frequencies. However, cost reduction benefits do not exceed equipment costs under all operations.

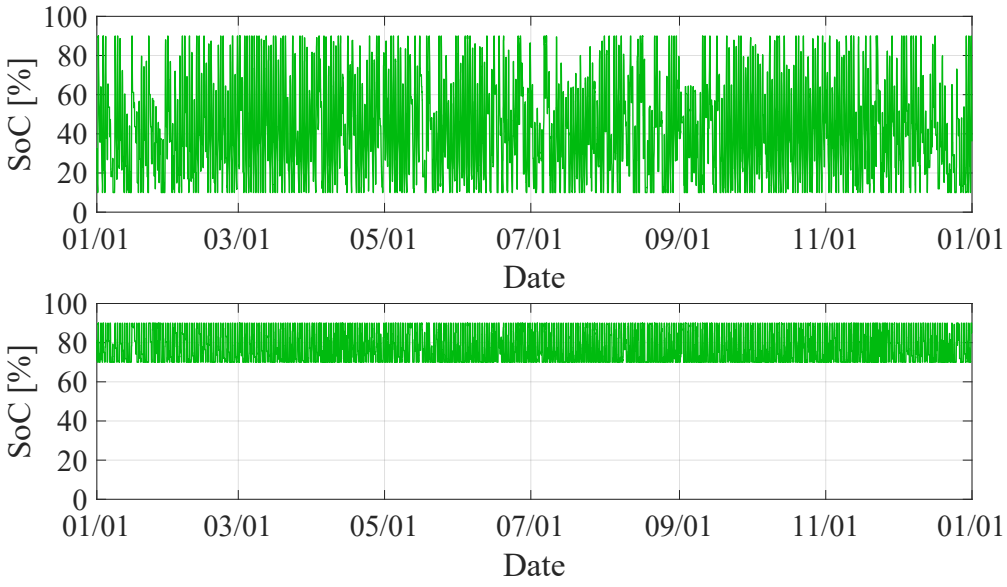

Figure 12. Annual SoC profile under the optimization without considering degradation in one household. Upper: margin 0%, lower: margin 60%.

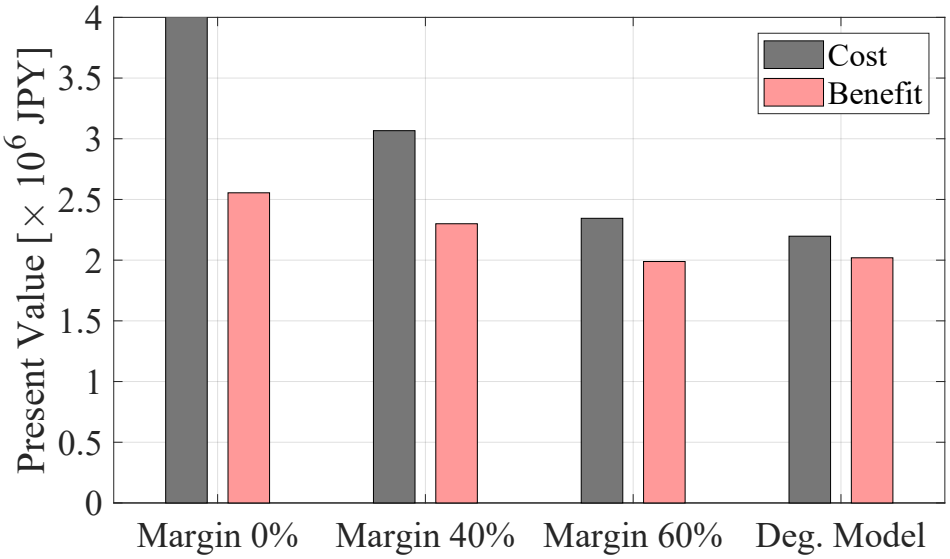

Figure 13. Comparison of net present values for equipment costs and cost reduction benefits in one household. "Deg. Model" indicates the optimization considering degradation.

Next, this paper compares the cost reduction benefits and equipment costs in 70 households. Figure 14 shows a comparison between cost reductions and equipment costs in 70 households. The horizontal axis shows the average of annual demand in one household. Benefits do not include outage mitigation. The cost reductions increase as household demand increases because of more self-consumptions. They exceed equipment costs in

2 households (2.9%) with a margin 60% and in 18 households (25.7%) with optimization considering degradation.

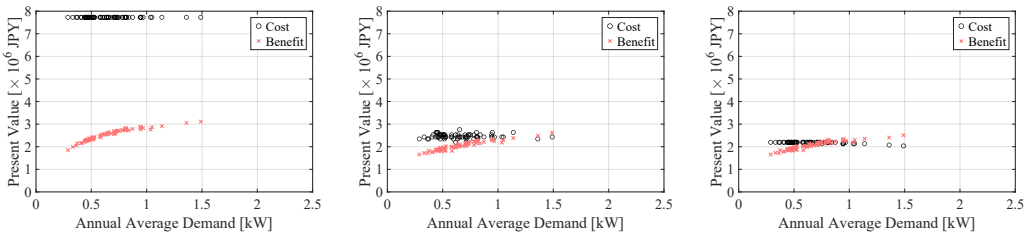

Figure 14. Comparison of net present values for equipment costs and cost reduction benefits in 70 households, categorized by annual average demand. (**Left**): margin 0%, (**Center**): margin 60%, (**Right**): optimization considering degradation.

Table 5. Annual electricity costs and battery degradation for one household. Cost differences are relative to the case without a PV/BESS system ("No PV/BESS"). Hyphens in "No PV/BESS" mean that this case shows the reference of costs and has no batteries. "Deg. Model" indicates the optimization considering degradation.

Case	Elec. Cost (Diff.) [JPY]	Degradation [%/Year]
No PV/BESS	225,500 (–)	–
Margin 0%	69,890 (−155,610)	9.55
Margin 40%	87,250 (−138,250)	2.88
Margin 60%	108,780 (−116,720)	1.93
Deg. Model	106,540 (−118,960)	1.67

3.2. Outage Simulation

This paper simulates operations during predictable and unpredictable outages in the summer using the rule-based algorithm. In unpredictable outages, the normal operation impacts the resilience because initial SoCs differ.

The program was written by MATLAB R2024b and executed by the same hardware as Section 3.1. It took around 30 min for the whole simulation using the plugged-in laptop using parallel computation with 4 threads.

First, mitigation of predictable outages is evaluated. Figure 15 shows the energy supplied to critical demand and the percent continuous supply hour in 70 households. There are 2208 scenarios in each household, and the figures show the mean energy supplied and the median and worst 5% of the continuous supply hour. The mean energy supplied ranges from 14 kWh to 26.7 kWh. It increases as the demand increases because of larger critical loads. The resilience metric, the percent continuous supply hour, also depends on the demand but is negatively related. Its median is larger than 60% (29 h) in all households. Looking at the worst 5% value, it ranges from 30% (14 h) to 100% (48 h). The battery's operation explains the relation between the demand and metric. The battery charges PV's excess generation in the daytime and discharges at night. Smaller demand results in more excess generation in the daytime and smaller critical loads at night. Thus, the battery can supply electricity overnight in smaller demand, leading to better resilience.

Next, mitigation of unpredictable outages is evaluated. The initial battery SoC varies in the normal operations. Thus, this paper compares operations among different optimizations. Figure 16 shows the mean energy supplied in 70 households. Compared to the predictable outage scenarios, the mean energy supplied decreases by up to 4 kWh because the battery has less energy. Figure 17 shows the median and worst 5% of the percent continuous supply hour in 70 households. In all operation cases, the metric decreases as the demand increases. This is because the battery supplies to larger critical loads, and its SoC runs out faster. The

normal operation also significantly impacts the metric. Under the operation with a margin of 0%, the worst 5% values reach 20% (9–10 h) in most of the households. In contrast, the worst 5% values achieve 30% (15 h) under the operations with a margin of 60% and considering degradation. This is because the battery sustains supply overnight even when an outage suddenly happens at night. After sunrise, PV generation allows the system to sustain supply. Thus, operations maintaining a high SoC improve supply continuity at the beginning of any outage.

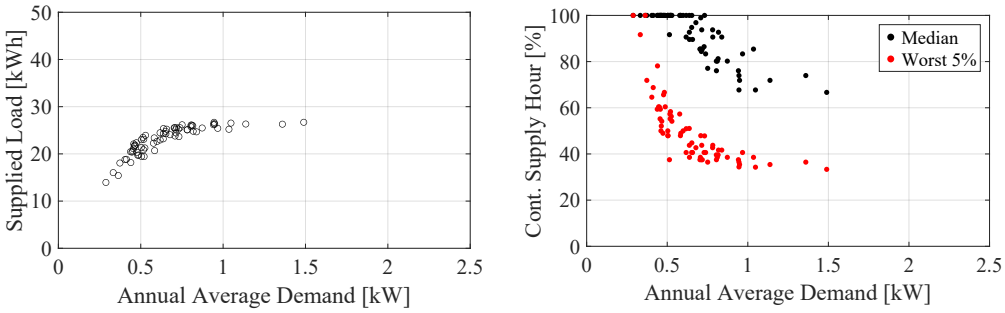

Figure 15. Outage mitigation during a 48 h predictable outage in the summer in each household. (**Left**): mean energy supplied, (**Right**): median and worst 5% of percent continuous supply hours.

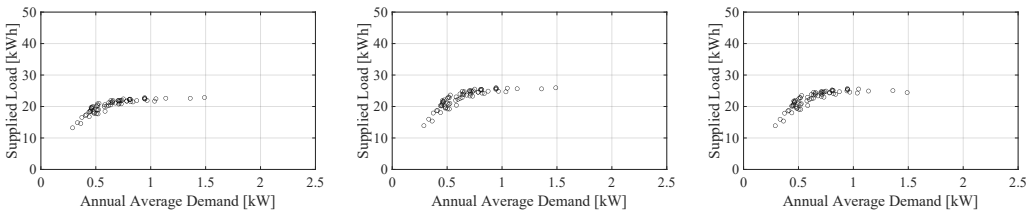

Figure 16. Mean energy supplied during a 48 h unpredictable outage in the summer in each household. (**Left**): margin 0%, (**Center**): margin 60%, (**Right**): optimization considering degradation.

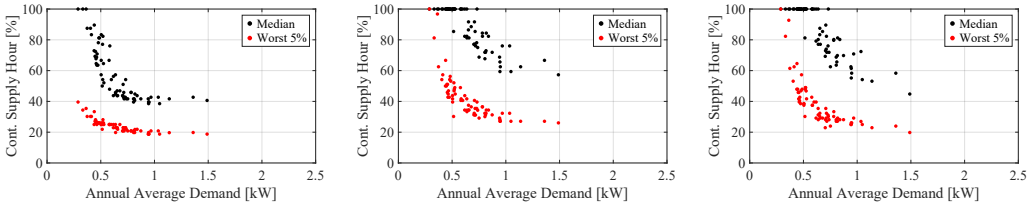

Figure 17. Median and worst 5% of percent continuous supply hours during a 48 h unpredictable outage in the summer in each household. (**Left**): margin 0%, (**Center**): margin 60%, (**Right**): optimization considering degradation.

To prepare for outages, the battery needs to deviate from its cost-optimal operation. It charges to ensure a sufficient SoC before predictable outages and to restore the cost-optimal SoC after them. Such operations increase electricity costs by 160–390 JPY per outage on average. Additionally, the battery deeply discharges during outages, accelerating its degradation. However, the maximum degradation during an outage is 7.8×10^{-2}%. Thus, even if supply shortages happen once in a year, the battery lifespan is shortened by about a year.

Winter outage mitigation is also simulated for comparison. Figure 18 shows the energy supplied to critical loads and the percent continuous supply hour during outages occurring from December to February. Compared with summer outages (see Figure 15), the energy supplied decreases in most households, ranging from 14.3 kWh to 22.6 kWh. The median of the percent continuous supply hours is also lower than in summer outages. This is because

PVs generate less electricity in winter than in summer (see Figure 3). Thus, PV/BESS systems supply less electricity during winter outages.

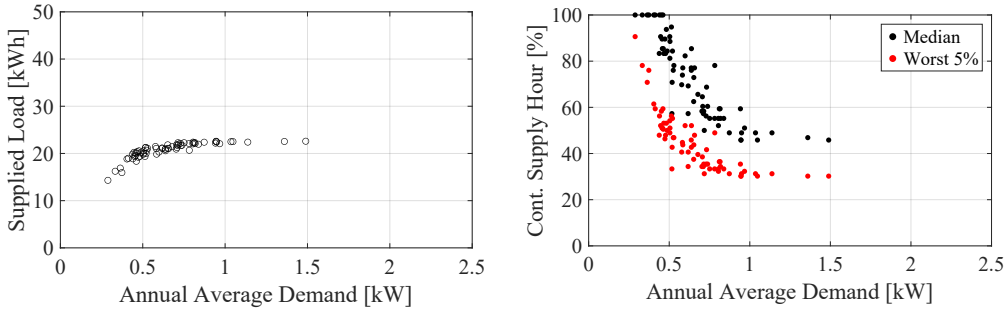

Figure 18. Outage mitigation during a 48 h predictable outage in the winter in each household. (**Left**): mean energy supplied, (**Right**): median and worst 5% of percent continuous supply hours.

3.3. Benefits with Outage Mitigation

This paper calculates the mean energy supplied during an outage. It is converted to benefits using a VoLL and outage frequency. This paper focuses on operations considering degradation. As shown in Figure 14, cost reductions do not exceed equipment costs in most households. However, the whole benefits including outage mitigation can exceed costs.

Cost reductions and outage mitigation vary in each household. Thus, this paper calculates the breakeven VoLL, demonstrating the minimum VoLL that the total benefit of PV/BESS systems exceeds their equipment costs. Figure 19 shows breakeven VoLLs in each household with different outage frequencies. Breakeven VoLLs negatively relate to the demand because smaller demand results in less cost savings and less energy supplied during outages. The maximum of breakeven VoLLs is around 18,100 JPY/kWh in the present outage frequency and around 7100 JPY/kWh in a larger frequency.

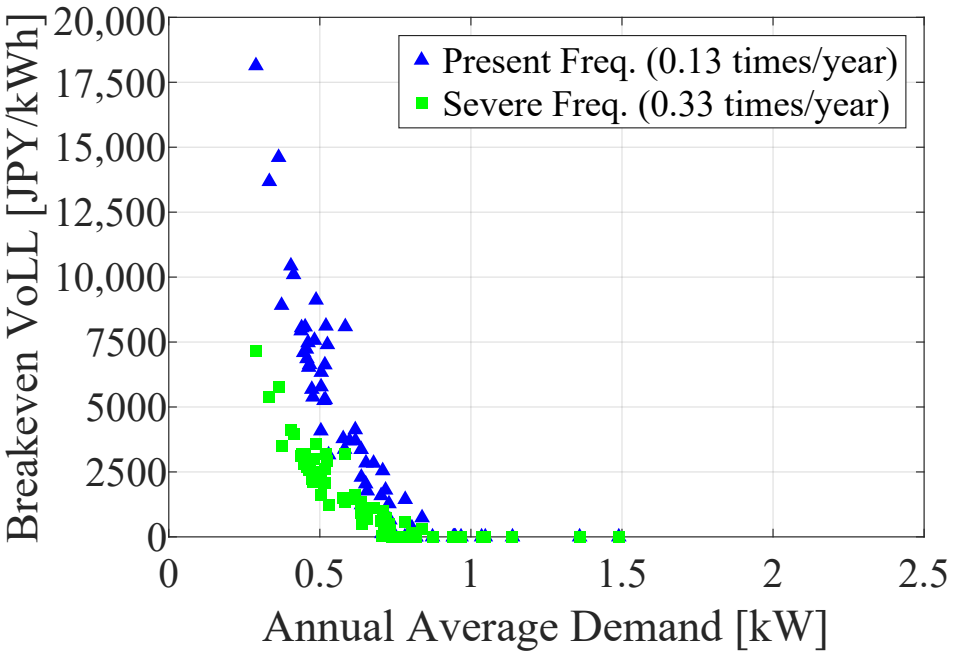

Figure 19. Breakeven VoLLs for 70 households under different outage frequencies, based on operations considering degradation. The frequency "0.13 times/year" reflects the historical average outage frequency per household, while "0.33 times/year" correspondes to the historical frequency of large-scale typhoon-induced outages.

Next, the expected proportion of households introducing the PV/BESS system is calculated by the VoLL distribution (see Figure 10). Table 6 shows the expected proportion

with different outage frequencies. Without the outage mitigation benefit, the proportion is 25.7%. The outage mitigation benefit increases the expected proportion by 12.2% points in the present outage frequency and 21.5% points in a larger frequency. Table 6 does not include degradation during outages, but it reduces the proportion by 0.4% points. This paper assumes that the VoLL is independent of household demand. If there is a positive correlation, the expected proportion can be lower because mitigation benefits for households with smaller demand will further decrease.

Table 6. Expected introduction of PV/BESS systems under operations considering degradation.

Outage Frequency	Total Proportion [%]
0	25.7
0.13 times/year	37.9
0.33 times/year	47.2

Gasoline generators are an alternative to batteries for outage mitigation. Their equipment cost (e.g., 250,000 JPY for 1.8 kVA and 3 h [69]) is significantly lower than that of the battery (1,210,000 JPY for 5 kW/13.5 kWh). Thus, photovoltaics and gasoline generators are more economical than PV/BESS systems, even when considering electricity cost reductions and outage mitigation. However, gasoline generators cannot utilize PV generation, whereas the battery enables synergies through increased self-consumption.

The result demonstrates that outage mitigation can stimulate introducing residential PV/BESS systems. At the same time, it is necessary to reduce electricity costs and extend battery lifespans for their introduction. The proposed operation considering degradation can help their introcution by sustaining cost reductions, extending lifespans, and mitigating severe outages.

4. Conclusions

The residential PV/BESS system is essential to tackle more frequent natural disasters and uncertainty of electricity prices. This paper aims to an operation of residential PV/BESS systems that balances electricity cost reduction, battery degradation, and outage mitigation. The optimization model determines normal operations by minimizing the sum of annual electricity costs and battery degradation costs, while maintaining a high SoC to enhance resilience. Additionally, this paper simulates operations during 48 h outages using the rule-based algorithm. The simulation evaluates energy supplied and supply continuity. The mitigation benefit is quantified through the distribution of residential VoLLs.

The results indicate that the proposed operation keeps the battery SoC higher than 50%, preventing intense degradation. For households with large electricity demand, cost reductions can exceed equipment costs, making PV/BESS adoption economically viable. Outage simulations show that the mean energy supplied during a 48 h outage ranges from 14 kWh to 26.7 kWh, depending on the demand. The resilience metric increases from 20% to 30% in severe situations under the proposed operation. Furthermore, incorporating outage mitigation benefits increases the proportion of households motivated to adopt PV/BESS systems from 25.7% to 47.2% with a frequent outage situation. Thus, the outage mitigation benefits motivate households to introduce the PV/BESS system. In conclusion, the proposed operation contributes to the economic efficiency of PV/BESS systems. It also improves supply continuity in outages regardless of their predictability.

Some households do not have enough incentive to introduce a PV/BESS system, especially when their demand is not large. They can be vulnerable to supply interruptions in power systems. Proposals of a system to enable them to access energy during outages are important for the resilient power system. Public facilities, such as evacuation sites, are

one of the keys to the system. We will further consider local systems to mitigate outage damage for more people.

This study evaluates supply continuity using the percent continuous supply hour. However, residential resilience encompasses additional factors, such as the initial response to outages and prolonged supply shortages. The ability to maintain supply at the onset of interruptions increases the likelihood of enduring them until external assistance becomes available. Prolonged shortages pose direct threats to life, such as rising indoor temperatures [44] and interruptions to medical equipment [45]. Integrating these aspects with the continuity metric will provide a more comprehensive assessment of household risk. Developing an integrated framework for resilience will be the focus of future work.

Author Contributions: Conceptualization, M.M. (Masashi Matsubara) and R.M.; methodology, M.M. (Masashi Matsubara); software, M.M. (Masashi Matsubara); validation, M.M. (Masashi Matsubara); formal analysis, M.M. (Masashi Matsubara); investigation, M.M. (Masashi Matsubara), M.M. (Masahiro Mae), and R.M.; resources, R.M.; data curation, M.M. (Masashi Matsubara); writing—original draft preparation, M.M. (Masashi Matsubara); writing—review and editing, M.M. (Masahiro Mae) and R.M.; visualization, M.M. (Masashi Matsubara); supervision, R.M.; project administration, R.M.; funding acquisition, R.M. All authors have read and agreed to the published version of the manuscript.

Funding: This research received no external funding.

Data Availability Statement: The anonymized data that support the findings of this paper are available on request from the corresponding author. The data are in a protected repository and are not publicly available to ensure privacy of households.

Conflicts of Interest: The authors declare no conflicts of interest.

References

1. Cabinet Office, Government of Japan. Special Feature: Catastrophic and Frequent Torrential Rain. In *White Paper on Disaster Management 2020*; Cabinet Office in Japan: Tokyo, Japan, 2020; pp. 6–10. Available online: https://www.bousai.go.jp/en/documentation/white_paper/pdf/2020/SF1-1.pdf (accessed on 20 November 2025).
2. Busby, J.W.; Baker, K.; Bazilian, M.D.; Gilbert, A.Q.; Grubert, E.; Rai, V.; Rhodes, J.D.; Shidore, S.; Smith, C.A.; Webber, M.E. Cascading risks: Understanding the 2021 winter blackout in Texas. *Energy Res. Soc. Sci.* **2021**, *77*, 102106. https://doi.org/10.1016/j.erss.2021.102106.
3. Aki, H. Demand-Side Resiliency and Electricity Continuity: Experiences and Lessons Learned in Japan. *Proc. IEEE* **2017**, *105*, 1443–1455. https://doi.org/10.1109/JPROC.2016.2633780.
4. Cabinet Office, Government of Japan. Special Feature: Consecutive Disasters –Toward the Establishment of a Disaster Conscious Society–. In *White Paper on Disaster Management 2019*; Cabinet Office in Japan: Tokyo, Japan, 2019; pp. 22–33. Available online: https://www.bousai.go.jp/en/documentation/white_paper/pdf/SF1-1.pdf (accessed on 20 November 2025).
5. Agency for Natural Resources and Energy, Japan. Energy White Paper 2024 (Summary) (FY2023 Annual Report on Energy). Available online: https://www.enecho.meti.go.jp/en/category/whitepaper/pdf/2024_outline.pdf (accessed on 20 November 2025).
6. IEA. World Energy Outlook 2024. Available online: https://www.iea.org/reports/world-energy-outlook-2024 (accessed on 20 November 2025).
7. Khezri, R.; Mahmoudi, A.; Aki, H. Optimal planning of solar photovoltaic and battery storage systems for grid-connected residential sector: Review, challenges and new perspectives. *Renew. Sustain. Energy Rev.* **2022**, *153*, 111763. https://doi.org/10.1016/j.rser.2021.111763.
8. Al Khafaf, N.; Rezaei, A.A.; Moradi Amani, A.; Jalili, M.; McGrath, B.; Meegahapola, L.; Vahidnia, A. Impact of battery storage on residential energy consumption: An Australian case study based on smart meter data. *Renew. Energy* **2022**, *182*, 390–400. https://doi.org/10.1016/j.renene.2021.10.005.
9. Honda, T.; Ozawa, A.; Wakamatsu, H. Profitability assessment of residential photovoltaic battery systems in japan using electric power big data. *Sustainability* **2021**, *13*, 5370. https://doi.org/10.3390/su13105370.
10. Huang, Z.; Wang, F.; Lu, Y.; Chen, X.; Wu, Q. Optimization model for home energy management system of rural dwellings. *Energy* **2023**, *283*, 129039. https://doi.org/10.1016/j.energy.2023.129039.

11. Tsai, C.T.; Ocampo, E.M.; Beza, T.M.; Kuo, C.C. Techno-Economic and Sizing Analysis of Battery Energy Storage System for Behind-the-Meter Application. *IEEE Access* **2020**, *8*, 203734–203746. https://doi.org/10.1109/ACCESS.2020.3036660.
12. Abdolmaleki, L.; Berardi, U. Hybrid solar energy systems with hydrogen and electrical energy storage for a single house and a midrise apartment in North America. *Int. J. Hydrogen Energy* **2024**, *52*, 1381–1394. https://doi.org/10.1016/j.ijhydene.2023.11.222.
13. Liu, Y.; Ma, J.; Xing, X.; Liu, X.; Wang, W. A home energy management system incorporating data-driven uncertainty-aware user preference. *Appl. Energy* **2022**, *326*, 119911. https://doi.org/10.1016/j.apenergy.2022.119911.
14. Uddin, K.; Gough, R.; Radcliffe, J.; Marco, J.; Jennings, P. Techno-economic analysis of the viability of residential photovoltaic systems using lithium-ion batteries for energy storage in the United Kingdom. *Appl. Energy* **2017**, *206*, 12–21. https://doi.org/10.1016/j.apenergy.2017.08.170.
15. Alramlawi, M.; Gabash, A.; Mohagheghi, E.; Li, P. Optimal operation of hybrid PV-battery system considering grid scheduled blackouts and battery lifetime. *Sol. Energy* **2018**, *161*, 125–137. https://doi.org/10.1016/j.solener.2017.12.022.
16. Amini, M.; Nazari, M.H.; Hosseinian, S.H. Optimal Scheduling and Cost-Benefit Analysis of Lithium-Ion Batteries Based on Battery State of Health. *IEEE Access* **2023**, *11*, 1359–1371. https://doi.org/10.1109/ACCESS.2022.3232282.
17. Wang, Y.; Chen, C.; Wang, J.; Baldick, R. Research on Resilience of Power Systems Under Natural Disasters—A Review. *IEEE Trans. Power Syst.* **2016**, *31*, 1604–1613. https://doi.org/10.1109/TPWRS.2015.2429656.
18. Nasri, A.; Abdollahi, A.; Rashidinejad, M. Multi-stage and resilience-based distribution network expansion planning against hurricanes based on vulnerability and resiliency metrics. *Int. J. Electr. Power Energy Syst.* **2022**, *136*, 107640. https://doi.org/10.1016/j.ijepes.2021.107640.
19. Moglen, R.L.; Barth, J.; Gupta, S.; Kawai, E.; Klise, K.; Leibowicz, B.D. A nexus approach to infrastructure resilience planning under uncertainty. *Reliab. Eng. Syst. Saf.* **2023**, *230*, 108931. https://doi.org/10.1016/j.ress.2022.108931.
20. Zhang, T.; Cialdea, S.; Orr, J.A.; Emanuel, A.E. Outage avoidance and amelioration using battery energy storage systems. *IEEE Trans. Ind. Appl.* **2016**, *52*, 5–10. https://doi.org/10.1109/TIA.2015.2461192.
21. Zhang, H.; Ma, S.; Ding, T.; Lin, Y.; Shahidehpour, M. Multi-Stage Multi-Zone Defender-Attacker-Defender Model for Optimal Resilience Strategy with Distribution Line Hardening and Energy Storage System Deployment. *IEEE Trans. Smart Grid* **2021**, *12*, 1194–1205. https://doi.org/10.1109/TSG.2020.3027767.
22. Wang, Z.; Zhang, L.; Tang, W.; Ma, Z.; Huang, J. Equilibrium configuration strategy of vehicle-to-grid-based electric vehicle charging stations in low-carbon resilient distribution networks. *Appl. Energy* **2024**, *361*, 122931. https://doi.org/10.1016/j.apenergy.2024.122931.
23. Guikema, S.D.; Davidson, R.A.; Liu, H. Statistical models of the effects of tree trimming on power system outages. *IEEE Trans. Power Deliv.* **2006**, *21*, 1549–1557. https://doi.org/10.1109/TPWRD.2005.860238.
24. Panteli, M.; Trakas, D.N.; Mancarella, P.; Hatziargyriou, N.D. Boosting the Power Grid Resilience to Extreme Weather Events Using Defensive Islanding. *IEEE Trans. Smart Grid* **2016**, *7*, 2913–2922. https://doi.org/10.1109/TSG.2016.2535228.
25. Panteli, M.; Mancarella, P.; Trakas, D.N.; Kyriakides, E.; Hatziargyriou, N.D. Metrics and Quantification of Operational and Infrastructure Resilience in Power Systems. *IEEE Trans. Power Syst.* **2017**, *32*, 4732–4742. https://doi.org/10.1109/TPWRS.2017.2664141.
26. Liu, X.; Shahidehpour, M.; Li, Z.; Liu, X.; Cao, Y.; Bie, Z. Microgrids for Enhancing the Power Grid Resilience in Extreme Conditions. *IEEE Trans. Smart Grid* **2017**, *8*, 589–597. https://doi.org/10.1109/TSG.2016.2579999.
27. Galvan, E.; Mandal, P.; Sang, Y. Networked microgrids with roof-top solar PV and battery energy storage to improve distribution grids resilience to natural disasters. *Int. J. Electr. Power Energy Syst.* **2020**, *123*, 106239. https://doi.org/10.1016/j.ijepes.2020.106239.
28. Roudbari, A.; Nateghi, A.; Yousefi-khanghah, B.; Asgharpour-Alamdari, H.; Zare, H. Resilience-oriented operation of smart grids by rescheduling of energy resources and electric vehicles management during extreme weather condition. *Sustain. Energy Grids Netw.* **2021**, *28*, 100547. https://doi.org/10.1016/j.segan.2021.100547.
29. An, S.; Qiu, J.; Lin, J.; Yao, Z.; Liang, Q.; Lu, X. Planning of a multi-agent mobile robot-based adaptive charging network for enhancing power system resilience under extreme conditions. *Appl. Energy* **2025**, *395*, 126252. https://doi.org/10.1016/j.apenergy.2025.126252.
30. Lei, S.; Chen, C.; Li, Y.; Hou, Y. Resilient Disaster Recovery Logistics of Distribution Systems: Co-Optimize Service Restoration with Repair Crew and Mobile Power Source Dispatch. *IEEE Trans. Smart Grid* **2019**, *10*, 6187–6202. https://doi.org/10.1109/TSG.2019.2899353.
31. Simpkins, T.; Anderson, K.; Cutler, D.; Olis, D. Optimal Sizing of a Solar-Plus-Storage System For Utility Bill Savings and Resiliency Benefits. In Proceedings of the 2016 IEEE Power & Energy Society Innovative Smart Grid Technologies Conference (ISGT), Minneapolis, MN, USA, 6–9 September 2016; Volume 9, pp. 1–6. https://doi.org/10.1109/ISGT.2016.7781237.
32. Gorman, W.; Barbose, G.; Miller, C.; White, P.; Carvallo, J.P.; Baik, S. Evaluating the potential for solar-plus-storage backup power in the United States as homes integrate efficient, flexible, and electrified energy technologies. *Energy* **2024**, *304*, 132180. https://doi.org/10.1016/j.energy.2024.132180.

33. Cole, W.; Greer, D.; Lamb, K. The potential for using local PV to meet critical loads during hurricanes. *Sol. Energy* **2020**, *205*, 37–43. https://doi.org/10.1016/j.solener.2020.04.094.
34. Kumar, N.M.; Ghosh, A.; Chopra, S.S. Power resilience enhancement of a residential electricity user using photovoltaics and a battery energy storage system under uncertainty conditions. *Energies* **2020**, *13*, 4193. https://doi.org/10.3390/en13164193.
35. Wang, J.; Qin, J.; Zhong, H.; Rajagopal, R.; Xia, Q.; Kang, C. Reliability Value of Distributed Solar+Storage Systems Amidst Rare Weather Events. *IEEE Trans. Smart Grid* **2019**, *10*, 4476–4486. https://doi.org/10.1109/TSG.2018.2861227.
36. Matsubara, M.; Mae, M.; Matsuhashi, R. Pilot Study on Residential Measures Against Unpredictable Outages with Batteries and Photovoltaics Considering Necessary Loads. In Proceedings of the 2024 20th International Conference on the European Energy Market (EEM), Istanbul, Turkiye, 10–12 June 2024; pp. 1–6. https://doi.org/10.1109/EEM60825.2024.10608987.
37. Yang, Y.; Wang, S. Resilient residential energy management with vehicle-to-home and photovoltaic uncertainty. *Int. J. Electr. Power Energy Syst.* **2021**, *132*, 107206. https://doi.org/10.1016/j.ijepes.2021.107206.
38. Liu, S.; Vlachokostas, A.; Kontou, E. Leveraging electric vehicles as a resiliency solution for residential backup power during outages. *Energy* **2025**, *318*, 134613. https://doi.org/10.1016/j.energy.2025.134613.
39. Iino, Y.; Hayashi, Y. Distributed coordinated energy management system for DERs to realize cooperative resilience against blackout of power grid. In Proceedings of the 2022 61st Annual Conference of the Society of Instrument and Control Engineers of Japan, SICE 2022, Kumamoto, Japan, 6–9 September 2022; pp. 75–80. https://doi.org/10.23919/SICE56594.2022.9905835.
40. Zhang, F.; Luo, F.; Dong, Z.; Liu, Y.; Ranzi, G. Hierarchical energy management scheme for residential communities under grid outage event. *IET Smart Grid* **2020**, *3*, 174–181. https://doi.org/10.1049/iet-stg.2019.0150.
41. Deng, Y.; Mu, Y.; Wang, X.; Jin, S.; He, K.; Jia, H.; Li, S.; Zhang, J. Two-stage residential community energy management utilizing EVs and household load flexibility under grid outage event. *Energy Rep.* **2023**, *9*, 337–344. https://doi.org/10.1016/j.egyr.2022.10.414.
42. Gorman, W.; Barbose, G.; Carvallo, J.P.; Baik, S.; Miller, C.; White, P.; Praprost, M. County-level assessment of behind-the-meter solar and storage to mitigate long duration power interruptions for residential customers. *Appl. Energy* **2023**, *342*, 121166. https://doi.org/10.1016/j.apenergy.2023.121166.
43. Deng, Y.; Luo, F.; Mu, Y. Multi-stage energy management framework for residential communities using aggregated flexible energy resources in planned power outages. *Int. J. Electr. Power Energy Syst.* **2025**, *166*, 110584. https://doi.org/10.1016/j.ijepes.2025.110584.
44. Amada, K.; Kim, J.; Inaba, M.; Akimoto, M.; Kashihara, S.; ichi Tanabe, S. Feasibility of staying at home in a net-zero energy house during summer power outages. *Energy Build.* **2022**, *273*, 112352. https://doi.org/10.1016/j.enbuild.2022.112352.
45. Iwata, F.; Fujimoto, Y.; Hayashi, Y. Residential Battery Storage System Sizing for the Medically Vulnerable from the Life Continuity Planning Perspective: Toward Economic Operation Using Uncertain Photovoltaic Output. *IEEJ Trans. Electr. Electron. Eng.* **2022**, *17*, 833–846. https://doi.org/10.1002/tee.23572.
46. Baik, S.; Sanstad, A.H.; Hanus, N.; Eto, J.H.; Larsen, P.H. A hybrid approach to estimating the economic value of power system resilience. *Electr. J.* **2021**, *34*, 107013. https://doi.org/10.1016/j.tej.2021.107013.
47. Gorman, W. The quest to quantify the value of lost load: A critical review of the economics of power outages. *Electr. J.* **2022**, *35*, 107187. https://doi.org/10.1016/j.tej.2022.107187.
48. Baik, S.; Davis, A.L.; Park, J.W.; Sirinterlikci, S.; Morgan, M.G. Estimating what US residential customers are willing to pay for resilience to large electricity outages of long duration. *Nat. Energy* **2020**, *5*, 250–258. https://doi.org/10.1038/s41560-020-0581-1.
49. Gorman, W.; Callaway, D. Do notifications affect households' willingness to pay to avoid power outages? Evidence from an experimental stated-preference survey in California. *Electr. J.* **2024**, *37*, 107385. https://doi.org/10.1016/j.tej.2024.107385.
50. Vennemo, H.; Rosnes, O.; Skulstad, A. The cost to households of a large electricity outage. *Energy Econ.* **2022**, *116*, 106394. https://doi.org/10.1016/J.ENECO.2022.106394.
51. Kim, K.; Nam, H.; Cho, Y. Estimation of the inconvenience cost of a rolling blackout in the residential sector: The case of South Korea. *Energy Policy* **2015**, *76*, 76–86. https://doi.org/10.1016/j.enpol.2014.10.020.
52. Matsubara, M.; Mae, M.; Matsuhashi, R. Investigation of Residential Value of Lost Load and the Importance of Electric Loads During Outages in Japan. *Energies* **2025**, *18*, 2060. https://doi.org/10.3390/en18082060.
53. Anderson, K.; Laws, N.D.; Marr, S.; Lisell, L.; Jimenez, T.; Case, T.; Li, X.; Lohmann, D.; Cutler, D. Quantifying and Monetizing Renewable Energy Resiliency. *Sustain.* **2018**, *10*, 933. https://doi.org/10.3390/su10040933.
54. Japan Meteorological Agency. Historical Weather Data and Download. https://www.data.jma.go.jp/risk/obsdl/index.php (accessed on 20 November 2025). (In Japanese)
55. Japan Electric Power Exchange. Market Data. Available online: https://www.jepx.jp/en/electricpower/market-data/spot/ (accessed on 20 November 2025).
56. Lam, L.; Bauer, P. Practical Capacity Fading Model for Li-Ion Battery Cells in Electric Vehicles. *IEEE Trans. Power Electron.* **2013**, *28*, 5910–5918. https://doi.org/10.1109/TPEL.2012.2235083.

57. Thingvad, A.; Marinelli, M. Influence of V2G Frequency Services and Driving on Electric Vehicles Battery Degradation in the Nordic Countries. In Proceedings of the Proceedings of EVS 31 & EVTeC 2018, Kobe, Japan, 1–3 October 2018; Volume 10.
58. Lee, J.O.; Kim, Y.S. Novel battery degradation cost formulation for optimal scheduling of battery energy storage systems. *Int. J. Electr. Power Energy Syst.* **2022**, *137*, 107795. https://doi.org/10.1016/j.ijepes.2021.107795.
59. Cabinet Office, Government of Japan. Disaster Information. Available online: https://www.bousai.go.jp/updates/index.html (accessed on 20 November 2025). (In Japanese)
60. Organization for Cross-Regional Coordination of Transmission Operators, Japan. Outlook for Electricity Supply and Demand-Actual Data for FY 2022-I. Actual Electric Supply and Demand. Available online: https://www.occto.or.jp/en/information_disclosure/annual_report/files/2023_annualreport_240131.pdf (accessed on 20 November 2025).
61. Federation of Electric Power Companies of Japan. Number of Customers for Lighting and Power demands. Available online: https://pdb.fepc.or.jp/pdb/%E4%B8%80%E8%88%AC_%E6%A4%9C%E7%B4%A2_%E9%9B%BB%E7%81%AF%E9%9B%BB%E5%8A%9B%E5%A5%91%E7%B4%84%E5%8F%A3%E6%95%B0_%E8%8B%B1%E8%AA%9E (accessed on 20 November 2025).
62. The Headquarters for Earthquake Research Promotion. Earthquake Occurring in the Nankai Trough. Available online: https://www.jishin.go.jp/regional_seismicity/rs_kaiko/k_nankai/ (accessed on 20 November 2025). (In Japanese)
63. Hao, K.; Ialnazov, D.; Yamashiki, Y. GIS Analysis of Solar PV Locations and Disaster Risk Areas in Japan. *Front. Sustain.* **2021**, *2*, 815986. https://doi.org/10.3389/frsus.2021.815986.
64. Li, A.; Wu, J. Quantitative assessment method of typhoon-induced photovoltaic damage and energy production losses: A case study of the 2024 Typhoon Yagi. *Geomat. Nat. Hazards Risk* **2025**, *16*, 2569795. https://doi.org/10.1080/19475705.2025.2569795.
65. Panteli, M.; Mancarella, P. The grid: Stronger, bigger, smarter?: Presenting a conceptual framework of power system resilience. *IEEE Power Energy Mag.* **2015**, *13*, 58–66. https://doi.org/10.1109/MPE.2015.2397334.
66. Bruneau, M.; Chang, S.E.; Eguchi, R.T.; Lee, G.C.; O'Rourke, T.D.; Reinhorn, A.M.; Shinozuka, M.; Tierney, K.; Wallace, W.A.; von Winterfeldt, D. A Framework to Quantitatively Assess and Enhance the Seismic Resilience of Communities. *Earthq. Spectra* **2003**, *19*, 733–752. https://doi.org/10.1193/1.1623497.
67. Jasiūnas, J.; Lund, P.D.; Mikkola, J. Energy system resilience – A review. *Renew. Sustain. Energy Rev.* **2021**, *150*, 111476. https://doi.org/10.1016/j.rser.2021.111476.
68. Chatterji, E.; Anderson, K.; Bazilian, M.D. Planning for a resilient home electricity supply system. *IEEE Access* **2021**, *9*, 133774–133785. https://doi.org/10.1109/ACCESS.2021.3116086.
69. Honda Power Equipment. Honda Generators: EU2200i Model. 2025. Available online: https://powerequipment.honda.com/generators/models/eu2200i (accessed on 4 December 2025).